Biochemical and Biophysical Research Communications 431 (2013) 86–91

Contents lists available at SciVerse ScienceDirect

Biochemical and Biophysical Research Communications

journal homepage: www.elsevier.com/locate/ybbrc

The NMR solution structure of the ubiquitin homology domain of Bcl-2-associated athanogene 1 (BAG-1-UBH) from *Mus musculus*

Hsiao-Wen Huang, C. Yu *

Department of Chemistry, National Tsing Hua University, Taiwan

ARTICLE INFO

Article history:
Received 12 December 2012
Available online 28 December 2012

Keywords:
Ubiquitin homology protein
Growth factor precursor
NMR solution structure
Protein–ligand interaction
Anti-apoptotic activity

ABSTRACT

BAG-1 (Bcl-2-associated athanogene 1), a multifunctional anti-apoptotic protein known to interact with various cellular proteins, was isolated using its interaction with the anti-apoptotic protein, Bcl-2. A 97-amino acid segment that includes the ubiquitin homology (UBH) domain of mouse BAG-1 (mBAG-1) interacts with a peptide corresponding to the cytoplasmic tail (CT) domain of proHB-EGF. This protein–peptide interaction is likely to have functional significance, as the two species exhibit a synergistic cytoprotective effect. In this study, we determined the solution structure of mBAG-1-UBH and investigated its interaction with the proHB-EGF-CT peptide using isothermal titration calorimetry and NMR spectroscopy. The solution structure of mBAG-1-UBH was shown to be similar to the previously reported structure of hBAG-1-UBH (PDB code 1WXV). However, their electrostatic potential maps demonstrated some differences in the UBH motifs that may be important for protein–peptide interaction. An NMR titration experiment demonstrated that residues 23–26 and residues 89–94 of mBAG-1-UBH are important for its molecular interaction with the peptide proHB-EGF-CT. BAG-1-UBH shares some biological functions with ubiquitin including the formation of polyubiquitin chain and the proteasomal protein degradation. The unique cytoprotective activity suggests mBAG-1-UBH to be an interesting ubiquitin-like protein with distinct biological functions. Here, we first reported the solution structure of mBAG-1-UBH and the growth factor precursor-interacting motif on the protein. For detail understanding about the binding interface and the mechanism of interaction, the study on mBAG-1-UBH/proHB-EGF-CT complex structure is necessary.

1. Introduction

The BAG (Bcl-2-associated athanogene) proteins (BAG-1, BAG-2, BAG-3, BAG-4 and BAG-5) share conserved C-terminal (the BAG domain) and central regions that bind to Hsc70/Hsp70 and Bcl-2, respectively, but they differ widely in their N-terminal domains. These proteins act as anti-apoptotic factors by inhibiting the chaperone activity of Hsc70/Hsp70 and by increasing the anti-cell death function of Bcl-2 [1]. The BAG-family proteins have been implicated in different cell processes linked to cell survival and have been found to be expressed at high levels in several types of tumor cell lines [2,3]. Thus, the over-expression of BAG-family proteins may serve as a novel molecular biomarker in diagnosing certain carcinomas.

BAG-1 (Bcl-2-associated athanogene 1) contains a unique ubiquitin homology (UBH) domain at its N-terminus that enables its interaction with the proteasome. The ability of BAG-1 to govern proteasomal degradation of certain proteins has been reported [4]. Furthermore, the binding between mouse BAG-1 and the membrane form of the heparin-binding EGF-like growth factor (HB-EGF) has been demonstrated [5]. HB-EGF, a potent mitogen and chemotactic factor for various cell types, localizes to the plasma membrane as a 20–30 kD precursor protein (proHB-EGF) containing an extracellular EGF-like domain, a transmembrane segment, and a short cytoplasmic tail (CT) [6]. Pull-down assays using domain constructs performed by Lin et al. identified the domain that interacts with proHB-EGF-CT as residues 1–97 of mBAG-1, an N-terminal fragment that includes its UBH domain. The UBH domain of mouse BAG-1 (residues 1–97) interacts with the 24-amino acid cytoplasmic tail of proHB-EGF and increases HB-EGF secretion, leading to cell survival [5]. The protein and peptide exhibit synergistic cytoprotective effects that are abolished in the presence of mBAG-1 or pro-HB-EGF alone. ProHB-EGF, Hsp70 and Bcl-2 interact with mBAG-1 at distinct binding domains, and thus, it is possible that mBAG-1 represents a link between the growth factor precursor and anti-apoptotic mechanisms.

The coordinates of the solution structure of human BAG-1-UBH have been deposited in Protein Data Bank (PDB) with accession

* Corresponding author. Address: Department of Chemistry National Tsing Hua University, No. 101, Section 2, Kuang-Fu Road, Hsinchu 30013, Taiwan, ROC. Fax: +886 35 711082.

E-mail addresses: d9623541@oz.nthu.edu.tw (H.-W. Huang), cyu.nthu@gmail.com (C. Yu).

0006-291X/$ - see front matter © 2013 Elsevier Inc. All rights reserved.
http://dx.doi.org/10.1016/j.bbrc.2012.12.082

code 1WXV. The mouse and human proteins share 70% sequence identity (Fig. 3D), and thus, their structures might be similar. However, a previous study showed that there are significant differences between the ^{15}N-^{1}H HSQC spectra of mBAG-1-UBH and hBAG-1-UBH [7], suggesting some differences in the chemical environments between the two structures.

The complete backbone and side chain resonances of mBAG-1-UBH were assigned previously by NMR spectroscopy [7]. In this study, we first determined the protein structure using solution NMR spectroscopy. To study its interaction with the proHB-EGF-CT peptide using HSQC titration and isothermal titration calorimetry (ITC) experiment, proHB-EGF-CT was cloned and overexpressed in *Escherichia coli* cell. The sequence information was included in Fig. 3D and the molecular weight of purified proHB-EGF-CT was confirmed by TOF-ESI mass (Supplementary Fig. 1). Circular dichroism (CD) study showed that the purified peptide is a random coil (Supplementary Fig. 2). The mBAG-1-UBH/proHB-EGF-CT interaction was represented as a one binding site model using ITC experiment. The stoichiometry of binding equals to one proHB-EGF-CT molecule per monomer of mBAG-1-UBH. We further identified the putative proHB-EGF-CT-binding site on mBAG-1-UBH by HSQC titrations. The binding motif comprises the C-terminus and the turn between β1 and β2 of mBAG-1-UBH which is different from the normal interaction surfaces on ubiquitin [8]. This finding suggests mBAG-1-UBH to be an interesting ubiquitin-like protein with distinct functional motif which is probably related to its cytoprotective activity.

2. Materials and methods

2.1. Protein/peptide expression and purification

The mBAG-1-UBH protein was expressed and purified as described previously [7]. NMR samples consisted of 0.5–1.0 mM ^{15}N- or ^{15}N/^{13}C-labeled mBAG-1-UBH in 20 mM PBS buffer (pH 6.0) containing 100 mM NaCl, 5 mM DTT, and 10% (v/v) D_2O (i.e., NMR buffer). The cDNA fragment encoding the peptide proHB-EGF-CT (residues 185–208) was subcloned into the vector pGEX-4T1. The plasmid was then transformed into *E. coli* BL21 (DE3) cells (Novagen) to express the recombinant fusion protein GST-proHB-EGF-CT. The unlabeled fusion protein was expressed in Luria Broth (LB) medium. After overnight growth, cultures were diluted 50-fold and incubated at 37 °C, 200 rpm until reaching an OD_{600} of 0.6. Protein expression was then induced with 0.2 mM isopropyl β-D-1-thiogalactopyranoside for 4 h at 37 °C, 200 rpm. The cells were harvested, and the bacterial pellet was resuspended in 20 mM PBS buffer (pH 7.3) containing 1 mM phenylmethylsulfonyl fluoride. After sonication and ultracentrifugation, the soluble GST-proHB-EGF-CT fusion protein, present in the supernatant of the cell lysate, was purified on a Glutathione Sepharose 4B column (GE). The GST fusion protein was eluted, and the tag was cleaved by addition of 1 unit thrombin per mg fusion protein. The GST tag was separated from the protein on a dC18 HPLC column (Atlantis). Fractions containing purified proHB-EGF-CT were collected, lyophilized and dissolved in 20 mM PBS buffer (pH 6.0) containing 100 mM NaCl and 5 mM DTT. The molecular weight of the purified peptide was confirmed by electrospray ionization mass spectrometry (Supplementary Fig. 1).

2.2. ^{1}H-^{15}N HSQC chemical shift perturbation experiments

The ^{1}H-^{15}N HSQC spectrum of a protein provides information about the chemical environment of each residue and allows fingerprinting of the conformation of the protein's backbone. ^{15}N-labeled mBAG-1-UBH and the unlabeled proHB-EGF-CT peptide were prepared in NMR buffer, and their ^{15}N-^{1}H HSQC spectra were recorded at 25 °C on a VARIAN-700 MHz NMR spectrometer equipped with a cold probe. Aliquots of a 1.5 mM solution of unlabeled proHB-EGF-CT were titrated into a 0.5 mM ^{15}N-labeled mBAG-1-UBH solution to obtain mixtures with 1:0, 1:0.5–1:3 ratios of mBAG-1-UBH:proHB-EGF-CT. An HSQC spectrum was recorded at each titration point.

2.3. Isothermal titration calorimetry

To study the interaction between mBAG-1-UBH and proHB-EGF-CT, an isothermal titration calorimetry (ITC) experiment was performed using a VP-ITC calorimeter (MicroCal). Both the protein and peptide samples were dissolved in 20 mM PBS buffer (pH 6.0) containing 100 mM NaCl. All experiments were performed at 25 °C. The calorimetry cell contained 1.4 ml of 0.015 mM mBAG-1-UBH, to which was titrated 240 μL of 0.134 mM proHB-EGF-CT. The titration curve was analyzed using ORIGIN 7.0 (OriginLab).

2.4. NMR spectroscopy

All NMR spectra were acquired at 25 °C on a VARIAN-700 MHz NMR spectrometer equipped with a cold probe. The ^{15}N-labeled and ^{15}N/^{13}C-labeled mBAG-1-UBH protein samples were prepared in NMR buffer to a final sample volume of approximately 500 μL and a final concentration of 1 mM. The 2 and 3D NMR experiments included ^{1}H-^{15}N HSQC, HNCO [9], HNCA [10], HN(CO)CA [11], HNCACB [12], HBHA(CO)NH [13], CC(CO)NH [14], HC(CO)NH [14], HCCH-TOCSY [15] and HCCH-COSY [16] were utilized for assignment of the backbone and side chain resonances as conducted previously [7]. NOE distance constraints were obtained from ^{15}N-edited NOESY-HSQC and ^{13}C-edited NOESY-HSQC spectra [17]. All NMR data were processed using the software VNMRJ and analyzed using the software SPARKY [18].

2.5. Structure calculation of mBAG-1-UBH

The input file for the mBAG-1-UBH structure calculation contained the distance restraints from the ^{15}N- and ^{13}C-edit NOESY spectra, the TALOS + -generated dihedral angle restraints based on the resonance assignments of ^{1}H, ^{15}N, $^{13}C_{\alpha}$, $^{13}C_{\beta}$ and ^{13}CO [19] and the distance restraints imposed by hydrogen bonds derived from CSI predictions [20]. The NOE cross peaks were automatically assigned, and peak intensities were iteratively converted to inter-proton distance restraints using the program ARIA [21]. The NOE assignments given in the first ARIA round were checked manually, with the unambiguous and ambiguous NOE restraints derived from ARIA outputs further analyzed and employed as inputs for the next

Table 1
Structural statistics for the final 20 simulated annealing structures of mBAG-1-UBH.

NMR Restraints for ARIA/CNS calculations Protein distance restraints	
Total	1237
Intraresidue	402
Sequential	261
Medium range	113
Long range	311
H-bond restraints	22
Dihedral angle restraints	128
Structural statistics for 20 structures	
Average rmsd (all residues)	
Backbone rmsd to mean (Å)	0.51 ± 0.07
Heavy atom rmsd to mean (Å)	0.96 ± 0.08
Average rmsd (structured region)	
Backbone rmsd to mean (Å)	0.21 ± 0.02
Heavy atom rmsd to mean (Å)	0.69 ± 0.07
Residues in the allowed region of the Ramachandran plot	97.4%

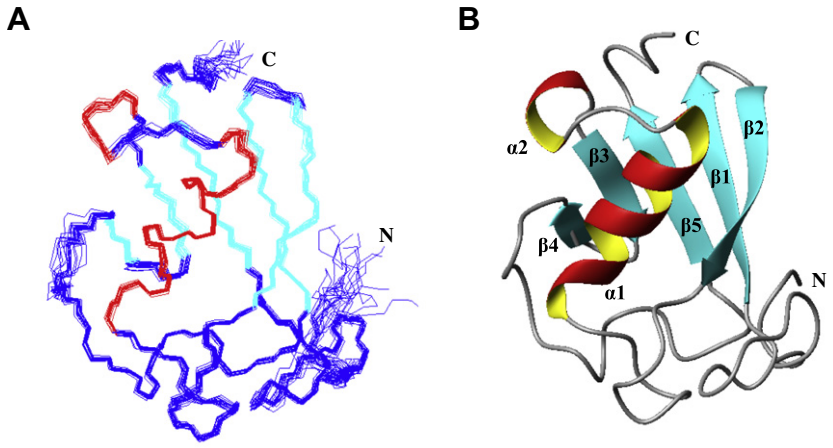

Fig. 1. Three-dimensional structure of mBAG-1-UBH determined by NMR spectroscopy (A) Superposition of the backbone atoms of the 20 final solution structures of mBAG-1-UBH. The structural regions are colored in red (α-helix) and cyan (β-sheet). (B) Ribbon representation of the tertiary structure of mBAG-1-UBH. The secondary structure elements are labeled. (For interpretation of the references to colour in this figure legend, the reader is referred to the web version of this article.)

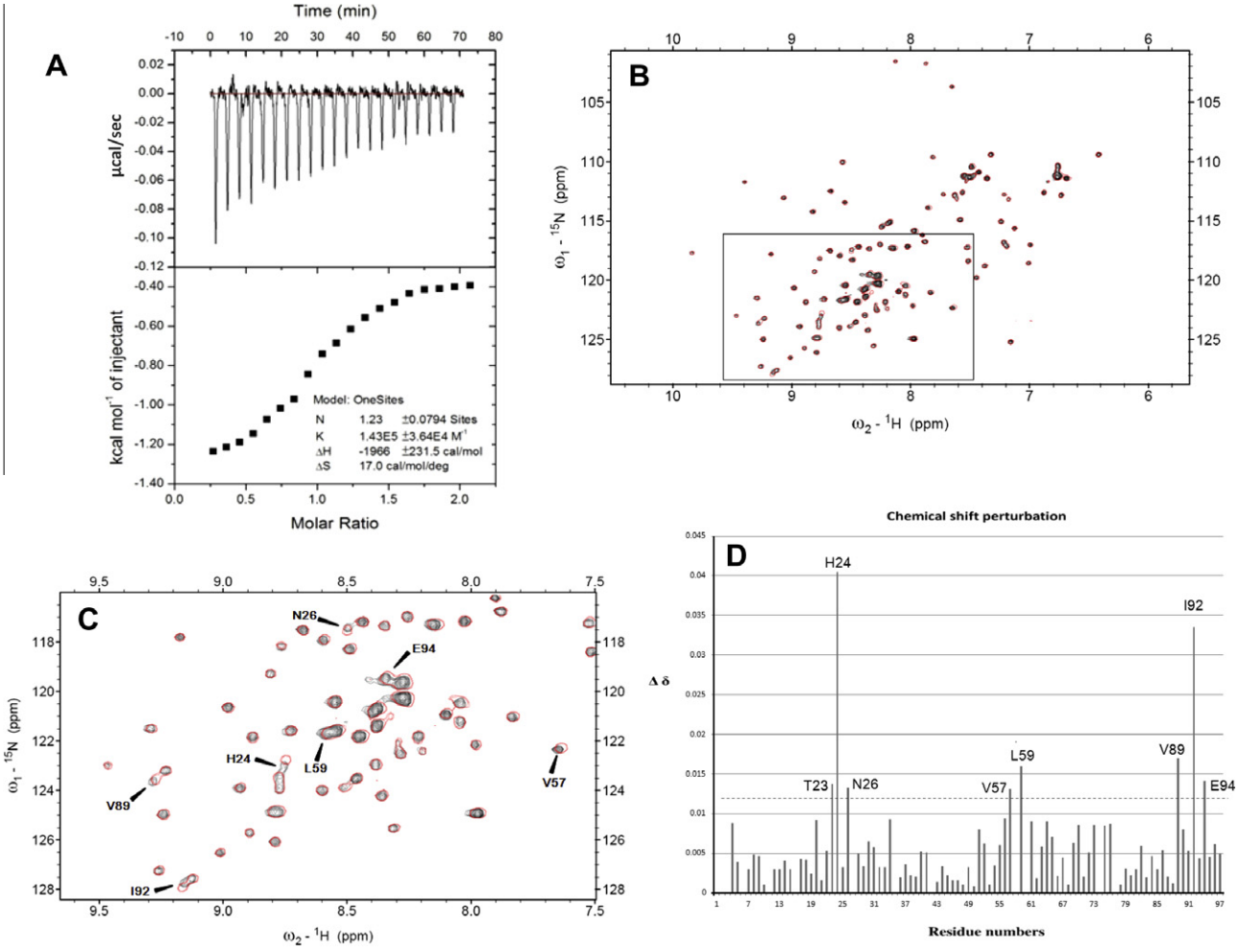

Fig. 2. Binding study between mBAG-1-UBH and proHB-EGF-CT (A) Isothermogram representing the binding of mBAG-1-UBH to proHB-EGF-CT at 25 °C. The binding constant for the mBAG-1-UBH/proHB-EGF-CT interaction is 6.9 µM. The raw data of the titration of mBAG-1-UBH with proHB-EGF-CT are shown in the upper panel, and the integrated data obtained after subtracting the heat of dilution are shown in the lower panel. The titrations were performed in 20 mM PBS buffer, pH 6.0, 100 mM NaCl. The concentrations of mBAG-1-UBH and HB-EGF-CT used in ITC experiments are 0.015 and 0.134 mM, respectively. (B) The overlaid 2D ^{1}H-^{15}N HSQC spectra highlight the differences between free mBAG-1-UBH (black) and proHB-EGF-CT-bound mBAG-1-UBH (red). (C) Magnified diagram of the boxed region in Fig. 2B. (D) Weighted average of ^{15}N and ^{1}H chemical shift perturbations of residues in mBAG-1-UBH induced by complex formation with proHB-EGF-CT. The dashed line is intended to indicate residues exhibiting significant chemical shift perturbations (>0.012 ppm). The residues T23, H24, N26, V57, L59, V89, I92 and E94 show the most significant chemical shift perturbations. (For interpretation of the references to colour in this figure legend, the reader is referred to the web version of this article.)

round of calculations. Two hundred structures were calculated using ARIA and were further refined in explicit solvent using CNS [22]. From this process, an ensemble of the 20 best structures with the lowest energies were obtained, and the qualities of these were analyzed by PROCHECK [23].

3. Results

3.1. Structure of mBAG-1-UBH

The structure of mBAG-1-UBH was determined using 1237 experimental and empirical NMR restraints, including 1087 NOE restraints, 22 hydrogen bond restraints and 128 dihedral angle restraints. A summary of the structure statistics for these 20 structures is given in Table 1. Analysis of a Ramachandran plot for the ensemble of 20 structures indicates that 97.4% of residues are in the allowed region. The root-mean-square deviation (RMSD) values for these structures were 0.69 ± 0.08 Å and 0.96 ± 0.07 Å for the heavy atoms of the structured regions and the full-length protein, respectively. The atomic coordinates and NMR-derived restraints of mBAG-1-UBH have been deposited in the PDB with accession code 2lwp. The solution structure of mBAG-1-UBH protein consists of 3.5 turns of an α-helix, containing residues 44–55; a short helical fragment, containing residues 59–61; and a mixed five-strand β-sheet (β1–5, shown in Fig. 1). Strands β1 and β5, composed of residues 19–24 and 88–92, respectively, are par-

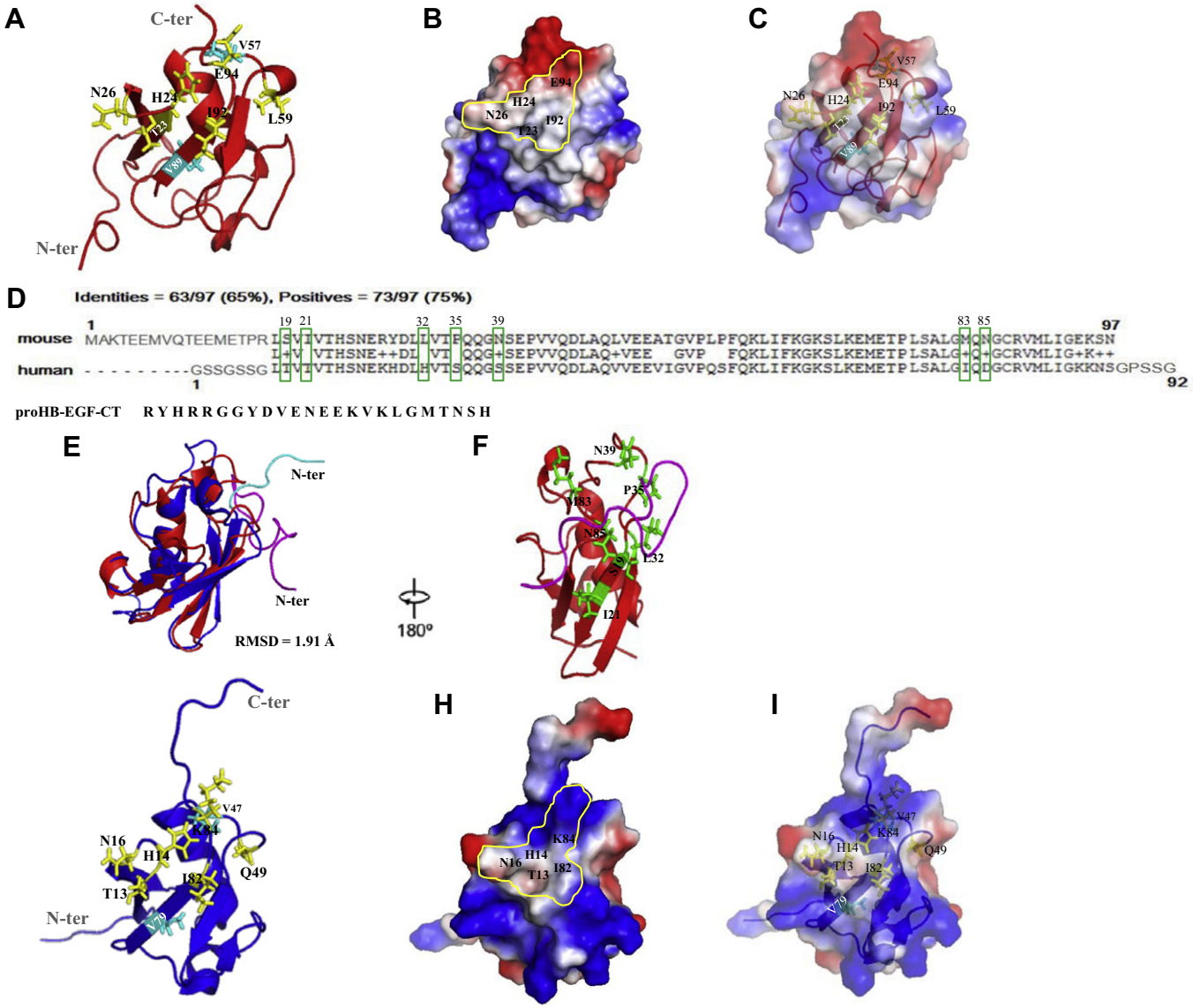

Fig. 3. Comparison of the solution structures of BAG-1-UBH from mouse and human (A) The names and numbers of side chains of the active (yellow sticks) and inactive (cyan sticks) residues affected upon proHB-EGF-CT binding are labeled in black in the NMR structure of mBAG-1-UBH. The putative proHB-EGF-CT-binding surface comprised of these active residues is encircled in yellow in (B) the electrostatic potential view and (C) the surface-transparent view. (D) The sequence of the proHB-EGF-CT peptide and the sequence alignment of mouse and human BAG-1-UBH, with the alignment result given on the second line. An identical residue is represented as its amino acid code, whereas a conserved substitution is labeled with a "+". Including conservative substitutions, the alignment reveals 65–75% similarity between mouse and human BAG-1-UBH sequences. (E) The overlaid solution structures of mBAG-1-UBH (red) and hBAG-1-UBH (blue) with their N-termini colored in pink (residues 1–17 in the mouse form) and cyan (residues 1–7 in the human form). The coordinates of the solution structure of hBAG-1-UBH are from PDB accession code 1WXV. The RMSD between these two structures is 2.85 Å. (F) The side chains of those residues (I21, S19, L32, P35, N39, M83 and N85) in mBAG-1-UBH that interact with its N-terminus are labeled in green sticks. These residues, which are not conserved between mouse and human BAG-1-UBH sequences, are indicated in the green boxes in Fig. 3D. (G) The affected resides based on the sequence alignment (Fig. 3D) are also labeled in the NMR structure of hBAG-1-UBH. The corresponding proHB-EGF-CT-binding surface (shown in the yellow circle) in (H) the electrostatic potential view of hBAG-1-UBH and (I) its surface-transparent view. (For interpretation of the references to colour in this figure legend, the reader is referred to the web version of this article.)

allel, whereas strands β2–4, composed of residues 27–32, 64–66 and 69–70, respectively, are anti-parallel in orientation.

3.2. Binding study between mBAG-1-UBH and proHB-EGF-CT

The protein mBAG-1-UBH was proposed to interact with the peptide proHB-EGF-CT based on immunoblotting and pull-down assays [5]. In this study, we used ITC and NMR chemical shift perturbation assays to investigate the protein–peptide interaction. The equilibrium dissociation constant was measured to be approximately 6.9 μM by ITC. The mBAG-1-UBH/proHB-EGF-CT interaction was represented as a one binding site model. The stoichiometry of binding equals to one proHB-EGF-CT molecule per monomer of mBAG-1-UBH (Fig. 2A). The chemical shift perturbations of ^{15}N-^{1}H cross peaks in the 2D ^{15}N-^{1}H HSQC spectrum induced upon addition of proHB-EGF-CT provide useful information for mapping the putative proHB-EGF-CT binding site on the mBAG-1-UBH protein. The cross peaks in the 2D HSQC spectrum of the mBAG-1-UBH that shift upon addition of increasing concentrations of proHB-EGF-CT became saturated at the 1:1 ratio (Supplementary Fig. 3). This indicates a 1:1 binding stoichiometry upon complex formation. Significant chemical shift perturbations were observed upon comparison of the ^{1}H-^{15}N HSQC spectra of free mBAG-1-UBH and of the mBAG-1-UBH/proHB-EGF-CT complex in a 1:1 M ratio (Fig. 2B and C). Particularly, residues T23, H24, N26, V57, L59, V89, I92 and E94 demonstrated significant chemical shift perturbations (Fig. 2D). Solvent-exposed (active) residues, including T23, H24, N26, L59, I92 and E94, were identified using NACCESS [24]. The affected active residues were then mapped onto the NMR structure of mBAG-1-UBH (Fig. 3A–C). As observed in the electrostatic potential map, all of the active residues, with the exception of L59, are located on the nearby surface (Fig. 3B, yellow circle), including one turn between the β1 and β2 strands and the C-terminus (Fig. 3A). These five active residues (T23, H24, N26, I92 and E94) were predicted to constitute the main binding site for the proHB-EGF-CT peptide.

3.3. Comparison of the solution structures of BAG-1-UBH from human and mouse

A high degree of sequence similarity (70%) was noted between mBAG-1-UBH and its human equivalent (PDB accession code 1WXV) (Fig. 3D). The distributions of secondary structural elements are similar between the two structures, with an RMSD of 1.91 Å over all the atoms in the structural regions (Fig. 3E). However, careful analysis revealed two significant differences between the structures of mouse and human BAG-1-UBH. The first major difference was in the folding of the N-terminus. The N-terminus of mouse BAG-1-UBH contains 10 additional residues, and this extension causes the N-terminal segment to fold back in contact with the protein, a feature that is not observed in human BAG-1-UBH. mBAG-1-UBH contains several residues (I21, S19, L32, P35, N39, M83 and N85) that interact with its N-terminus but that are not conserved in the human form (Fig. 3F). The actual NOE cross-peaks to argue the close proximity between the N-terminus and the residues that are important for this interaction was presented in (Supplementary Fig. 4. Second, the electrostatic potential surface for the proHB-EGF-CT binding site is quite different in mBAG-1-UBH relative to the corresponding area on the human form. These perturbed residues were also mapped onto the NMR structure of hBAG-1-UBH (Fig. 3G). There are predominantly neutral and negatively charged residues around the proHB-EGF-CT binding site on the surface of mBAG-1-UBH, (Fig. 3B and C) compared to the neutral and positively charged residues around the corresponding region of hBAG-1-UBH (Fig. 3H and I).

4. Discussion

The N-terminal ubiquitin homology domain (UBH) of BAG-1 is important in signaling proteasomal degradation and in the regulation of cell growth. A regulatory function has been reported for the chaperone cofactor at the interface between protein folding and protein degradation [25]. In this study, we determined the solution structure of the mBAG-1-UBH protein using NMR spectroscopy. Using existing structural information and these NMR assignments, it is possible to design future experimental and modeling studies to examine the role of mBAG-1-UBH in cell survival regulation. Additionally, we mapped the interactions between mBAG-1-UBH and proHB-EGF-CT. Although the chemical shift perturbations in the 2D ^{15}N-^{1}H HSQC spectrum of mBAG-1-UBH induced upon proHB-EGF-CT addition are rather small, from 0.013 to 0.04 ppm (Fig. 2D), previously reported biological assays [5] and our ITC data confirm this protein–peptide interaction. The small chemical shift perturbations induced by proHB-EGF-CT binding to mBAG-1-UBH indicate that the structure of the latter species was not significantly perturbed. The residues involved in the interaction with proHB-EGF-CT were located primarily in the region around a turn separating the β1 and β2 strands and the C-terminus of mBAG-1-UBH (Fig. 3A). This surface consists mainly of neutral and negatively charged residues, including E94 (Fig. 3B and C), suggesting that hydrophobic and electrostatic interactions are the likely forces that are involved in the interaction between proHB-EGF-CT and mBAG-1-UBH.

Our NMR structure of mBAG-1-UBH showed similar structural arrangement to the solution structure of hBAG-1-UBH in the PDB (code 1WXV), except for the folding of N-terminus (Fig. 3E and F). This similarity is consistent with the high sequence identity (70%) between the two proteins. However, the peptide-interacting motif on the mBAG-1-UBH protein is distinct from that of the human form, as determined by analysis of the electrostatic potential maps of the two structures (Fig. 3B and H). The five active residues (T23, H24, N26, I92 and E94) that likely constitute the proHB-EGF-CT binding site in mBAG-1-UBH are conserved in the human form, with the exception of E94, which corresponds to K84 in hBAG-1-UBH. The oppositely charged residues (E94 and K84 on mBAG-1-UBH and hBAG-1-UBH, respectively) likely interfere with the binding ability of proHB-EGF-CT, a peptide rich in basic residues. The distinct surface features of mBAG-1-UBH revealed in this study suggest that this protein may have unique functions relative to hBAG-1-UBH. Future work will include study of the protein–peptide binary complex in an attempt to understand the mechanism of interaction at the molecular level.

Acknowledgments

This work is supported by a Grant from the National Science Council (NSC) Taiwan (NSC100-2113-M007-012-MY3).

Appendix A. Supplementary data

Supplementary data associated with this article can be found, in the online version, at http://dx.doi.org/10.1016/j.bbrc.2012.12.082.

References

[1] S. Takayama, Z. Xie, J.C. Reed, An evolutionarily conserved family of Hsp70/Hsc70 molecular chaperone regulators, Journal of Biological Chemistry 274 (1999) 781–786.

[2] A. Batistatou, P. Kyzas, A. Goussia, E. Arkoumani, S. Voulgaris, K. Polyzoidis, N. Agnantis, D. Stefanou, Estrogen receptor beta (ERβ) protein expression correlates with BAG-1 and prognosis in brain glial tumours, Journal of Neuro-Oncology 77 (2006) 17–23.

[3] N.K. Clemo, T.J. Collard, S.L. Southern, K.D. Edwards, M. Moorghen, G. Packham, A. Hague, C. Paraskeva, A.C. Williams, BAG-1 is up-regulated in colorectal tumour progression and promotes colorectal tumour cell survival through increased NF-κB activity, Carcinogenesis 29 (2008) 849–857.
[4] F. Tsukahara, Y. Maru, Bag1 directly routes immature BCR-ABL for proteasomal degradation, Blood 116 (2010) 3582–3592.
[5] J. Lin, L. Hutchinson, S.M. Gaston, G. Raab, M.R. Freeman, BAG-1 is a novel cytoplasmic binding partner of the membrane form of heparin-binding EGF-like growth factor, Journal of Biological Chemistry 276 (2001) 30127–30132.
[6] M. Hieda, M. Isokane, M. Koizumi, C. Higashi, T. Tachibana, M. Shudou, T. Taguchi, Y. Hieda, S. Higashiyama, Membrane-anchored growth factor, HB-EGF, on the cell surface targeted to the inner nuclear membrane, the journal of cell biology 180 (2008) 763–769.
[7] H.-W. Huang, C. Yu, Backbone and side-chain resonance assignments (^{1}H, ^{15}N and ^{13}C) of the ubiquitin homology domain of mouse BAG-1, Biomolecular NMR Assignments (2012) 1–5.
[8] L. Hicke, H.L. Schubert, C.P. Hill, Ubiquitin-binding domains, Nature reviews. Molecular cell biology 6 (2005) 610–621.
[9] D.R. Muhandiram, L.E. Kay, Gradient-enhanced triple-resonance three-dimensional NMR experiments with improved sensitivity, Journal of Magnetic Resonance, Series B 103 (1994) 203–216.
[10] M. Ikura, L.E. Kay, A. Bax, A novel approach for sequential assignment of proton, carbon-13, and nitrogen-15 spectra of larger proteins: heteronuclear triple-resonance three-dimensional NMR spectroscopy, Application to calmodulin, Biochemistry 29 (1990) 4659–4667.
[11] A. Bax, M. Ikura, An efficient 3D NMR technique for correlating the proton and^{15}N backbone amide resonances with the α-carbon of the preceding residue in uniformly^{15}N/^{13}C enriched proteins, Journal of Biomolecular NMR 1 (1991) 99–104.
[12] M. Wittekind, L. Mueller, HNCACB, a high-sensitivity 3D NMR experiment to correlate amide-proton and nitrogen resonances with the alpha- and beta-carbon resonances in proteins, Journal of Magnetic Resonance, Series B 101 (1993) 201–205.
[13] S. Grzesiek, A. Bax, Amino acid type determination in the sequential assignment procedure of uniformly ^{13}C/^{15}N-enriched proteins, Journal of Biomolecular NMR 3 (1993) 185–204.
[14] S. Grzesiek, J. Anglister, A. Bax, Correlation of backbone amide and aliphatic side-chain resonances in ^{13}C/^{15}N-enriched proteins by isotropic mixing of ^{13}C magnetization, Journal of Magnetic Resonance, Series B 101 (1993) 114–119.
[15] A. Bax, G.M. Clore, A.M. Gronenborn, ^{1}H□^{1}H correlation via isotropic mixing of ^{13}C magnetization, a new three-dimensional approach for assigning ^{1}H and ^{13}C spectra of ^{13}C-enriched proteins, Journal of Magnetic Resonance 88 (1990) (1969) 425–431.
[16] A. Bax, G.M. Clore, P.C. Driscoll, A.M. Gronenborn, M. Ikura, L.E. Kay, Practical aspects of proton-carbon-carbon-proton three-dimensional correlation spectroscopy of ^{13}C-labeled proteins, Journal of Magnetic Resonance 87 (1990) (1969) 620–627.
[17] D. Marion, P.C. Driscoll, L.E. Kay, P.T. Wingfield, A. Bax, A.M. Gronenborn, G.M. Clore, Overcoming the overlap problem in the assignment of proton NMR spectra of larger proteins by use of three-dimensional heteronuclear proton-nitrogen-15 Hartmann-Hahn-multiple quantum coherence and nuclear Overhauser-multiple quantum coherence spectroscopy: application to interleukin 1.beta, Biochemistry 28 (1989) 6150–6156.
[18] T.D. Goddard, D.G. Kneller, SPARKY 3, University of California, San Francisco, http://www.cgl.ucsf.edu/home/sparky/.
[19] Y. Shen, F. Delaglio, G. Cornilescu, A. Bax, TALOS+: a hybrid method for predicting protein backbone torsion angles from NMR chemical shifts, Journal of Biomolecular NMR 44 (2009) 213–223.
[20] D.S. Wishart, B.D. Sykes, The ^{13}C chemical-shift index: a simple method for the identification of protein secondary structure using ^{13}C chemical-shift data, Journal of biomolecular NMR 4 (1994) 171–180.
[21] W. Rieping, M. Habeck, B. Bardiaux, A. Bernard, T.E. Malliavin, M. Nilges, ARIA2: automated NOE assignment and data integration in NMR structure calculation, Bioinformatics 23 (2007) 381–382.
[22] A.T. Brünger, P.D. Adams, G.M. Clore, W.L. DeLano, P. Gros, R.W. Grosse-Kunstleve, J.S. Jiang, J. Kuszewski, M. Nilges, N.S. Pannu, R.J. Read, L.M. Rice, T. Simonson, G.L. Warren, Crystallography & NMR system: a new software suite for macromolecular structure determination, acta crystallogr., Acta Crystallographica Section D: Biological Crystallography 54 (1998) 905–921.
[23] R.A. Laskowski, J.A. Rullmannn, M.W. MacArthur, R. Kaptein, J.M. Thornton, AQUA and PROCHECK-NMR: programs for checking the quality of protein structures solved by NMR, Journal of biomolecular NMR 8 (1996) 477–486.
[24] S.J. Hubbard, J.M. Thornton, 'NACCESS', Computer Program, Department of Biochemistry and Molecular Biology, University College London, 1993.
[25] J. Luders, J. Demand, J. Höhfeld, The ubiquitin-related BAG-1 provides a link between the molecular chaperones Hsc70/Hsp70 and the proteasome, Journal of Biological Chemistry 275 (2000) 4613–4617.